Atmospheric Environment 145 (2016) 19–28

Contents lists available at ScienceDirect

Atmospheric Environment

journal homepage: www.elsevier.com/locate/atmosenv

Near-source grid-based measurement of CO and PM2.5 concentration during a full-scale fire experiment in southern European shrubland

J.H. Amorim [a, *, 1], J. Valente [a], P. Cascão [a, 2], L.M. Ribeiro [b], D.X. Viegas [b], R. Ottmar [c], A.I. Miranda [a]

[a] CESAM & Department of Environment and Planning, University of Aveiro, 3810-193, Aveiro, Portugal
[b] Association for the Development of Industrial Aerodynamics, University of Coimbra, 3031-601, Coimbra, Portugal
[c] Pacific Wildland Fire Sciences Laboratory, U.S. Forest Service Pacific Northwest, Research Station, Seattle, WA, USA

HIGHLIGHTS

- Dynamics of wildland firefighters' exposure to smoke still scarcely understood.
- Grid of portable sensors allows detailed monitoring of near-source smoke levels.
- Individual exposure largely impacted by extreme spatial concentration gradients.
- Critical risk of acute exposure during smouldering.
- Visual estimate of fire safety conditions potentially misleading.

ARTICLE INFO

Article history:
Received 16 May 2016
Received in revised form
8 September 2016
Accepted 10 September 2016
Available online 12 September 2016

Keywords:
Fire experiments
Smoke emissions
Smoke plume
Firefighter exposure
Fire safety
Portable sensor

ABSTRACT

There is limited research on the exposure of wildland firefighters to smoke because of the operational obstacles when monitoring air pollutants in the field. In this work, a grid of portable sensors was used to measure PM2.5 and CO concentrations in the near-source region during the burn of two shrubland research blocks in Central Portugal. Strong spatial variability of smoke levels was observed in the analysis of the ratios between mean concentrations of neighbouring sensors, with values as high as 4.4 for PM2.5 and 7.4 for CO. These large gradients were registered at a distance of only 5 m suggesting that considerable differences on individual exposure can occur depending on the location of that individual in relation to the smoke plume trajectory. Also, peak events of 2–3 times the mean were observed in periods exceeding 6 min. In the two experiments, the average concentrations of both PM2.5 and CO were higher during smouldering, which represents a risk of acute exposure due to the closer proximity of firefighters to the emission source during mop-up, stressing the importance of wearing portable gas detectors for managing critical exposure. The collected data constitutes a step forward in the effort to understand the mechanisms controlling the exposure during firefighting operations, by providing a source of information on near-ground concentration fluctuations within a biomass-burning smoke plume at a fine spatial-temporal resolution.

© 2016 Elsevier Ltd. All rights reserved.

1. Introduction

Forest fires are a large source of air pollutants that may lead to environmental and human impacts. At the operational level, firefighters are often confronted with a smoky and toxic atmosphere with reduced visibility. In this context, the constituents of smoke can potentially have significant effects on the safety and health of personnel (e.g., Reinhardt and Ottmar, 2004; Miranda et al., 2010, 2012). The complex mixture of smoke constituents may induce adverse health effects such as acute and instantaneous eye and

* Corresponding author.
E-mail addresses: jorge.amorim@smhi.se (J.H. Amorim), joanavalente@ua.pt (J. Valente), pedro.cascao@ecotech.com (P. Cascão), luis.mario@adai.pt (L.M. Ribeiro), xavier.viegas@dem.uc.pt (D.X. Viegas), rottmar@fs.fed.us (R. Ottmar), miranda@ua.pt (A.I. Miranda).
[1] Present address: Swedish Meteorological and Hydrological Institute (SMHI), Air Quality Research Unit, SE-60176, Norrköping, Sweden.
[2] Present address: Ecotech Pty Ltd, Knoxfield, Victoria, 3180, Australia.

http://dx.doi.org/10.1016/j.atmosenv.2016.09.017
1352-2310/© 2016 Elsevier Ltd. All rights reserved.

respiratory irritation and shortness of breath. These health effects can lead to headaches, dizziness and nausea, and mild impairment of lung function that may last for hours or days (Reinhardt et al., 2000). Long-term effects are characterised by impaired respiratory function, increased risk of cancer, and cardiovascular disease (Rothman et al., 1991). The exposure to respirable particles and potentially toxic compounds adsorbed by the particles, such as polycyclic aromatic hydrocarbons (PAHs) and semivolatile organic compounds, are of increased concern since some may be carcinogenic (LeMasters et al., 2006; Youakim, 2006; IARC, 2010a), which led the International Agency for Research on Cancer (IARC) to classify the occupational exposure of a firefighter as possibly carcinogenic (IARC, 2010b).

There are a number of factors that affect the impacts of smoke on firefighter's health, including the concentration of specific air pollutants within the breathing zone, the exposure duration, the exertion levels, and the individual susceptibility (e.g., pre-existing lung or heart diseases) (Reisen and Brown, 2009). The composition of smoke itself depends on several other factors, such as the characteristics of the vegetation consumed, the efficiency of combustion, the fuel moisture content, fire temperature, and the weather conditions (e.g., Crutzen and Andreae, 1990; Levine, 1999; Ottmar et al., 2009). Despite the smoke exposure research studies carried out in the United States of America (Reinhardt et al., 2000; Reinhardt and Ottmar, 2000, 2004), Australia (McMahon and Bush, 1992; Materna et al., 1993; De Vos et al., 2009; Reisen and Brown, 2009; Reisen et al., 2011), Canada (Austin, 2008) and Portugal (Miranda et al., 2005, 2010, 2012), the current state of knowledge in this field is still limited. The inherent difficulty of monitoring smoke and personal exposure levels during a fire has contributed to this scientific gap.

To establish cause/effect relationships between fire activity, exposure to smoke and the effect on firefighter's health, a better understanding of the smoke plume dynamics in the near-source region is needed. In this context, the main goal of this work is to evaluate the spatial and temporal variation of the concentration of particles smaller than 2.5 μm in aerodynamic diameter (PM2.5) and carbon monoxide (CO) in the vicinity of the emission source during experimental bushfires, and how this translates into human safety issues during firefighting operations. This paper provides a source of information on near-ground concentration fluctuations within a smoke plume at a fine spatial-temporal resolution.

2. Site description and methods

The fire experiments were performed on May 6, 2010, on two research blocks in the mountain range of Lousã, Central Portugal (40° 15′N, 8° 10′W), at an elevation of approximately 1000 m. This area, known as 'Gestosa', has been an important field laboratory for over 20 years on the study of fire and its impacts, including smoke emissions, air quality and human exposure (Miranda et al., 2005, 2010, 2012; Viegas et al., 2002, 2006). Average physical characteristics of the burn blocks and vegetation are given in Table 1.

Meteorological observations were collected with an automated weather station and a 3 m high measurement mast positioned at approximately 150 m from the research blocks.

The fire ignition procedure was not meant to replicate a realistic fire scenario, but to create a consistent smoke plume that could be tracked by the ground sensors, while guaranteeing the safety of personnel and equipment during the experiments. In both research blocks the ignition pattern consisted of a line of fire along the top borders of the blocks, followed by a downhill linear ignition along the lateral borders. In block 2 there was an additional ignition at the lower corner that substantially increased the propagation. No fire suppression (direct or indirect attack) was used during the experiments. Table 2 summarizes the chronological sequence of the most significant events.

The technical characteristics of the portable monitoring equipment used for measuring the spatiotemporal dynamics of PM2.5 and CO concentration are detailed in Table 3. All the equipment was previously calibrated at the laboratory. In the case of SidePack AM510 sensors, the default calibration factor (standard ISO 12,103, A1 Test Dust) was applied for the determination of concentration. This test dust has a wide size distribution that averages the effect of particle size dependence on the measured signal and, therefore, is considered to be representative of a wide variety of ambient aerosols (TSI, 2012). Notwithstanding, similar instruments using real-time photometric technology have been shown to over-report PM levels in different wood smoke environments in comparison to gravimetric or filter-based methods (McNamara et al., 2011), and thus measurements should be interpreted with caution.

The position of the sensors in each research block is shown in Fig. 1. The grid layout was defined according to the prevailing wind during the burn to facilitate the capture of the smoke plume close to the fire and at ground level. The purpose of defining fixed positions for the sensors is to provide a better understanding of the spatial gradients of smoke levels in the near-source region of a fire, and not to measure the exposure of individuals in activity, as in previous papers by the authors (Miranda et al., 2010, 2012). The sensors were distributed around the higher section of the blocks at intervals of approximately 5 m. The first line of sensors distanced 5 m from the block border, and each line was roughly 5 m apart.

Each sensor was fixed to a mast at approximately 1.7 m above ground, as shown in Fig. 2, representing the average breathing zone of a firefighter.

3. Results and discussion

In the following sub-sections the data monitored in the two blocks is analysed in terms of: (3.1) meteorology, (3.2) fire behaviour, (3.3) smoke plume behaviour, and (3.4) air pollutant levels.

Table 2
Chronological description of the fire experiments (t is the local time and Δt is the elapsed time after ignition). Flaming and smouldering were differentiated by the analysis of infrared (IR) camera footage taken from an opposite hill.

Event	Block 1		Block 2	
	t (hh:mm)	Δ*t* (min)	*t* (hh:mm)	Δ*t* (min)
Fire ignition	09:56	0	11:25	0
End of flaming stage	10:30	34	11:31	6
End of smouldering stage	10:50	54	12:00	35

Table 1
Physical characteristics of the burn blocks. Fuel moisture was sampled 40 min before the first fire ignition.

Research block	Area (m^2)	Avg. slope (°)	Fuel cover (%)	Avg. fuel height (m)	Avg. fuel load (t ha^{-1})	Avg. fuel moisture (%)	Fuel species
1	1853	16	67	0.31	32.50	Live: 46.6	*Erica umbellata, Erica australis, Ulex minor, Chamaespartium tridentatum*
2	1743	18	105	0.68	35.50	Dead: 9.0	

Table 3
Technical specifications of the sensors.

Pollutant	Equipment	Sensor type	Number of sensors	Acquisition frequency	Time averaging	Range	Resolution
PM2.5	Personal Aerosol Monitor SidePack AM510 (TSI®)	90° light scattering, 670 nm laser diode	10	60 s	60 s	0 −20 mg m^{-3}	0.001 mg m^{-3}
CO	GasAlertExtreme (BW Technologies®)	Plug-in electrochemical cells	8	5 s	60 s	0 −1000 ppm	1 ppm

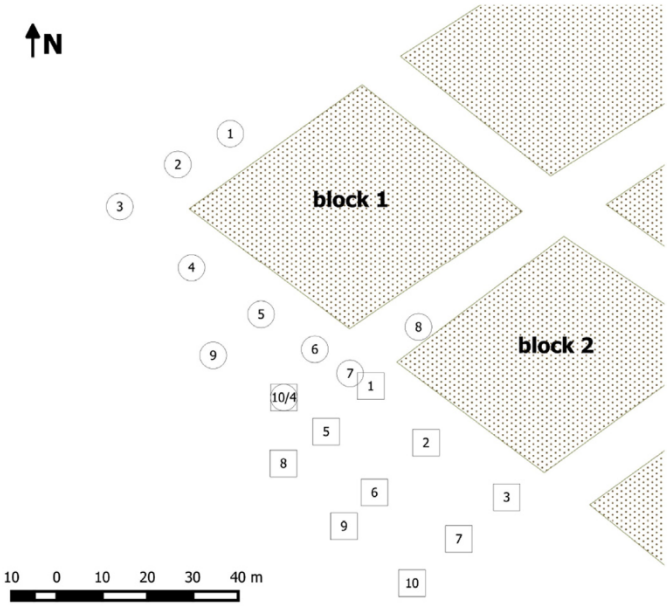

Fig. 1. Sensors grid layout (note that sensor 10 in block 1 and sensor 4 in block 2 share the same position). The terrain altitude increases from NE to SW.

Fig. 2. Mast mounted sensors during the fire experiments (photo taken during the burn of block 2).

3.1. Meteorological conditions

Average meteorological data acquired during the burns are shown in Table 4 and corresponding time variation in Fig. 3. The weather conditions were reasonably stable, despite a progressive decrease of mean wind velocity, accompanied by more intense fluctuation in block 2 and a rotation from East to Southeast. Despite this shift, the wind was consistently uphill during the experiments.

3.2. Fire behaviour

Fire descriptors such as rate of spread, flame length and height or linear intensity of the fire front are usually used to characterize fire behaviour. In this particular case, as there were multiple ignitions, it was not possible to measure or estimate rate of spread, but the characteristics of the flame can be analysed through the analysis of collected photographs, videos and infrared imagery.

The fire line intensity equation by Byram (1959) shows that:

$$I = H \times w \times r \quad (1)$$

Where, I is the fire intensity (kW.m^{-1}), H the fuel low heat of combustion (kJ.kg^{-1}), w the weight of fuel consumed per unit area (kg.m^{-2}), and r stands for the rate of spread (m.sec^{-1}). This expression can be adapted to use flame length (L) as a variable to calculate fire intensity (Rothermel and Deeming, 1980):

$$I = 258 \times L^{2.17} \quad (2)$$

For field observations, equation (2) can be rounded to a rough rule of thumb (Beck et al., 2002) according to:

$$I = 300 \times L^{2} \quad (3)$$

Equation (3) was used to estimate linear fire intensity. A visual analysis was performed on photographs, videos and IR images, using as reference for scale other elements with known dimensions, such as the block dimensions, trees, persons or fire trucks. The analysis was performed in different time instants and evenly throughout the blocks. The descriptive statistics are shown in Table 5.

There is a great dispersion of intensity values that has to do, firstly with an uneven fire propagation (as described earlier the goal was to produce a well-defined smoke plume), and secondly to the fact that the flame length estimations were taken all across the block, at different time instants, in order to make an estimation that was representative of the whole burn test. Block 1 had a downslope fire during most part of the test, hence the significantly lower intensity values observed. Standard deviation is consistently very high in relation to the mean value suggesting the complex dynamics of the burning conditions.

A data clustering by 5 classes based on intensity values was

Table 4
Observed meteorological data during the experiments: mean and standard deviation (±).

Block	Time period (hh:mm)	Wind velocity (m.s^{-1})	Wind direction (°)	Air temperature (°C)	Air humidity (%)
1	09:56–10:50	2.85 ± 0.63	95.8 ± 15.6	12.7 ± 0.5	45.7 ± 1.5
2	11:25–12:00	1.42 ± 1.09	129.0 ± 26.8	14.8 ± 0.7	38.3 ± 1.2

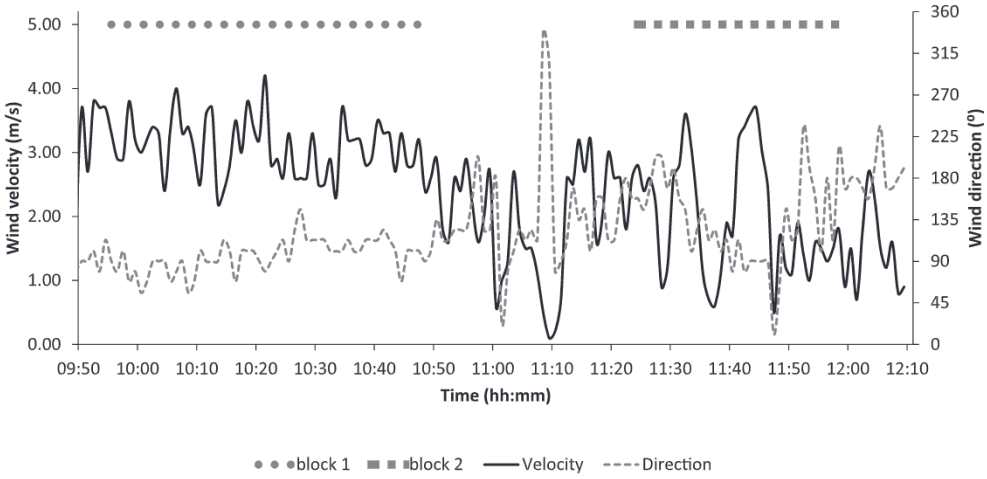

Fig. 3. Time evolution of 1 min averaged wind velocity and direction during the experiments.

Table 5
Descriptive statistics of the fire line intensity (I) estimation. Block borders indicated by their orientation ("N" is the number of measurements and "Range" the difference between minimum and maximum calculated intensity).

Block	Fire line position	I (kw.m^{-1})					
		N	Range	Minimum	Maximum	Mean	Std. Dev.
1	Downslope fire line	140	3511	32	3543	637	761
2	SE border – fire line	35	25,798	154	25,952	3264	5390
	SW border – fire line	12	13,513	346	13,859	3647	4185
	N corner – spot fire	7	10,941	154	11,095	4058	3861

Table 6
Coefficients for the regression models, in the form [PM2.5] = a × [CO] + b.

Block	Stage of fire	*a*	*b*	R^2	Number of observations
1	Total	0.783	0.219	0.69***	437
1	Flaming	0.783	0.175	0.76***	270
1	Smouldering	0.769	0.306	0.59***	167
2	Total	0.666	0.469	0.55***	285
2	Flaming	1.109	0.228	0.30***	55
2	Smouldering	0.639	0.564	0.55***	230

Signif. codes: '***' p-value < 0.0001.

performed following the classification presented by Alexander and Lanoville (1989) and ranging from "low" to "extreme" frontal fire intensity. The results are shown in Fig. 4.

Higher intensity values (larger than 10,000 kW m^{-1}) were estimated for the fire lines in the SE and SW borders of block 2, as indicated in Fig. 4. It is also confirmed the much higher fire intensity in block 2, leading to an average burning rate of 290 m^2 min^{-1}, against only 62 m^2 min^{-1} in block 1.

3.3. Smoke plume behaviour

Because of the fire ignition strategy, the moderate uphill wind registered during the experiments (below 4 m s^{-1}, in general) caused the deflection of the buoyant plume, allowing the sensors to be immersed in smoke during the full duration of the experiments (Fig. 5a). The decreased heat release in the smouldering stage is evidenced by the diminishing of plume rise in Fig. 5b.

In block 2, a fire spot was ignited at 11:28 close to the lower border, which rapidly propagated uphill with a very high intensity (Fig. 6a), creating a strong convective cell and a secondary buoyant plume characterised by a significantly high rise (Fig. 6b).

3.4. PM2.5 and CO concentrations

3.4.1. Spatial gradients

Fig. 7 shows the concentration acquired in each sensor normalized by the average of concentrations for all the sensors during the entire duration of each burn. The analysis of normalized values instead of absolute concentrations avoids the uncertainty associated with the use of a calibration factor as representative of a smoke aerosol, given the dynamic combustion conditions that determine the properties of the emitted particles. However, as indicative values, one can add that the mean PM2.5 concentration was 4.7 mg m^{-3} and 3.5 mg m^{-3}, and the mean CO level was 20.6 ppm and 34.4 ppm, respectively in blocks 1 and 2.

Results in Fig. 7 indicate strong crosswind concentration gradients from the central axis (sensors 5, 6 and 9 in block 1, and 2 and 5 in block 2) to the sides of the plume. This is related to a 'stable' wind direction, especially during the first experiment. For these atmospheric conditions, the entrainment of air from cleaner regions in the lateral boundaries of the plume creates a zone of lesser smoke close to the fire. However, this region is also characterised by strong concentration gradients between neighbouring locations located in the external plume boundary that can potentially induce critical conditions for firefighters. Sensors 6 and 7 in block 1 point this out as they were only 5 m apart and the ratio between mean concentrations during the essay equalled 4.4 and 7.4 for PM2.5 and CO, respectively. This effect is particularly noted during smouldering phase, when 1 min concentration ratios between close sensors (6 and 7) attained values as high as 8.1 for PM2.5 and 13.9 for CO.

Another aspect to consider is that although the peripheral side of the main plume trajectory can potentially offer lower mean exposure to smoke contaminants, occasional peaks (with variable intensity and duration) will determine the overall exposure risk. As

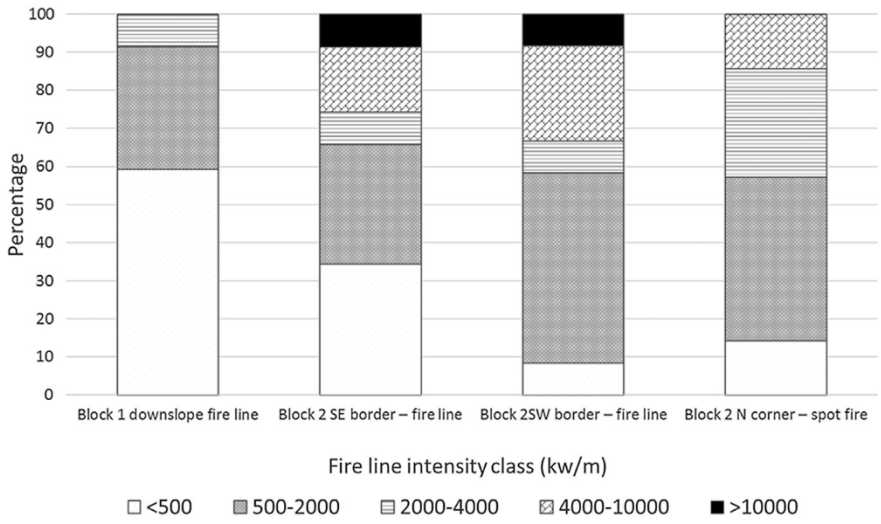

Fig. 4. Graphical distribution of percentage frequency of intensity values per class.

Fig. 5. Smoke plume structure during the burning of block 1 at (a) 10:14 and (b) 10:32 (start of the smouldering stage).

Fig. 6. Combined photo and IR image (colorscale indicating flames temperature) shortly after the point ignition (a) and smoke plume rise during smouldering (b).

seen in the analysis of sensors 1 and 2 in Figs. 7a and 1 min peak ratios (outmost outliers) of nearly 4 times the global average of the block were measured.

The instability of the atmospheric environment close to the fire is revealed in the fluctuation of the normalized concentrations. Extreme differences in standard deviation are found for CO in the second experiment between sensor 5 with 2.4 and sensor 10 registering only 0.3. In general, the farther the distance (aligned with the plume trajectory) to the emission source, the smaller the spread of the values around the mean.

An interesting feature in the comparison of both pollutants is the higher normalized peak levels for CO, which is particularly evident in block 1. Here, 75% of the CO sensors surpass a peak of 4, against only 10% for the PM2.5 sensors. This is related to different effects of turbulent mixing on particulate and gaseous pollutants and their behaviour in the near-source region.

In Fig. 8 the observations were sorted by concentration range and the corresponding duration of continuous events.

As expected, lower background concentrations persist for longer periods of time than episodic peak levels. A relevant conclusion

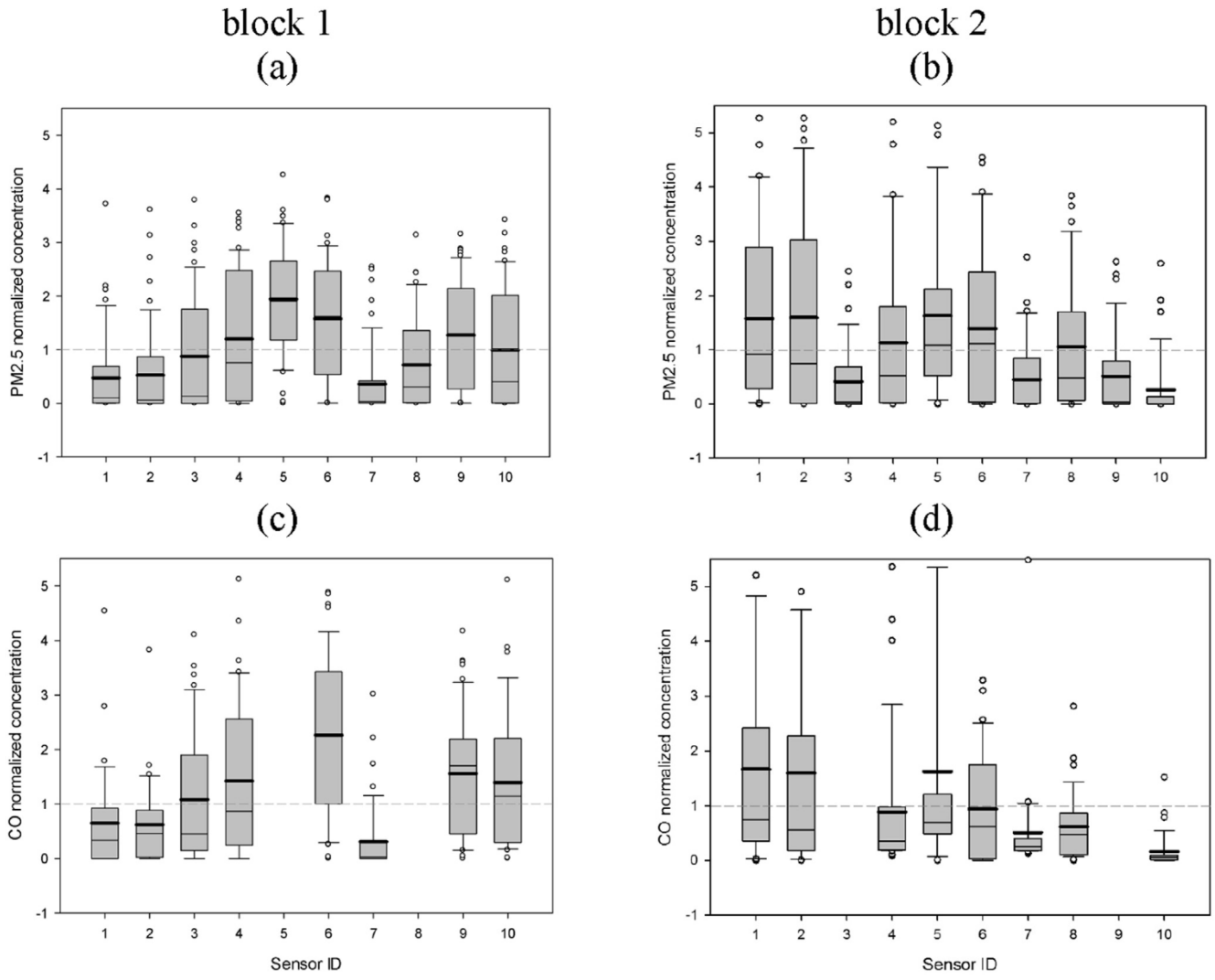

Fig. 7. Box plot of normalized 1 min averaged PM2.5 and CO concentration measured in each sensor in blocks 1 and 2. Thick lines show the sample means while thin lines represent the medians; box limits indicate the 25th and 75th percentiles; whiskers extend 1.5 times the interquartile range from the 25th and 75th percentiles; and outliers are represented by dots.

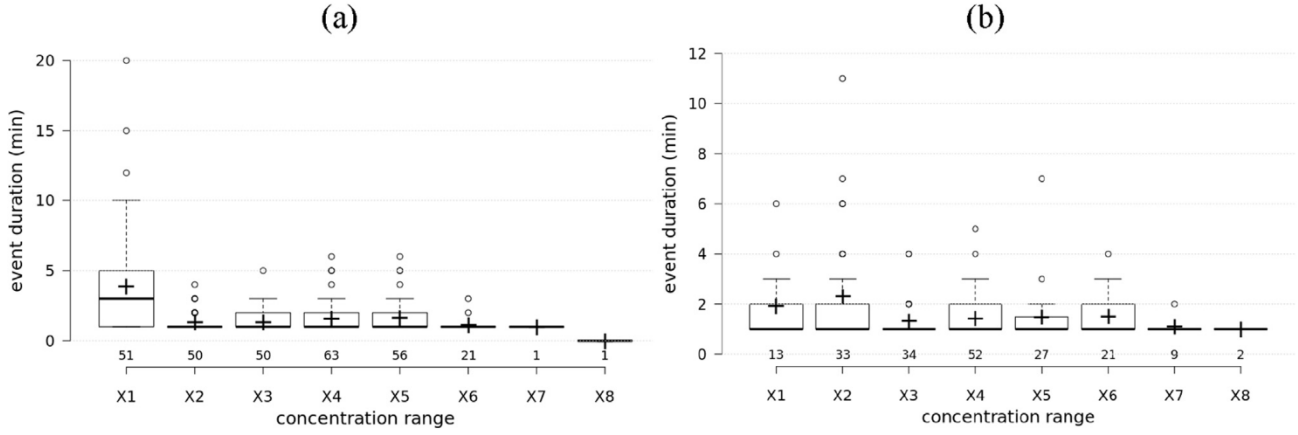

Fig. 8. Event duration per concentration range (X1 =]0,0.1μ[; X2 = [0.1μ,0.5μ[; X3 = [0.5μ,μ[; X4 = [μ,2μ[; X5 = [2μ,3μ[; X6 = [3μ,4μ[; X7 = [4μ,5μ[; X8 = [5μ,∞[, where μ is the average per block and pollutant) for (a) PM2.5 and CO (b). Centre lines show the medians; box limits indicate the 25th and 75th percentiles; whiskers extend 1.5 times the interquartile range from the 25th and 75th percentiles; outliers are represented by dots; and crosses represent sample means. Number of sample points indicated in the x-axis.

from Fig. 8 is that, for both pollutants, values as high as 2 to 3 times the mean (range X5) can extend continuously in time for more than 6 min. Despite the similar trends for both pollutants there is a clear distinction for lower concentrations (below 50% of the mean), with a tendency for very low PM2.5 levels (lower than 10% of the mean, i.e., X1) to persist longer (3rd quartile of 5 min and outmost outlier of 20 min).

3.4.2. Time evolution

The analysis of the time evolution of normalized concentrations (Fig. 9) can give a better perspective on the influence of the fire combustion stage.

In block 1, the decrease of PM2.5 (Fig. 9a) and CO (Fig. 9c) concentrations around 10:26 corresponds to the diminishing of flames intensity (that finally collapse at 10:30), thus revealing two distinct fire stages. The levels monitored during the first 30 min are a combination of both flaming and smouldering emissions, while the second peak in concentration (around 10:36) is exclusively caused by smouldering emissions. The much faster and higher intensity fire registered in block 2 was hardly captured by measurements during the flaming stage (before 11:31 in Fig. 9b and d), whereas the distinctive peak at 11:40 reveals the important contribution of smouldering to the overall air quality levels during a fire event. Despite in block 2 a strong gradient in PM2.5 average concentration was found in the transition from flaming to smouldering (from 1.0 to 4.0 mg m^{-3}, respectively), in the first burn the mean concentration in the two stages was almost identical (4.5 and 4.9 mg m^{-3}). It should be mentioned, however, that as a consequence of the stronger plume rise during flaming (as already discussed in the analysis of section 3.3), a tendency for the sensors to capture primarily the less buoyant regions of the smoke plume can occur during this stage. The same is to say that, in the field, the aerosol sampled during flaming can primarily be originated from smouldering emissions occurring in parallel with flaming. The

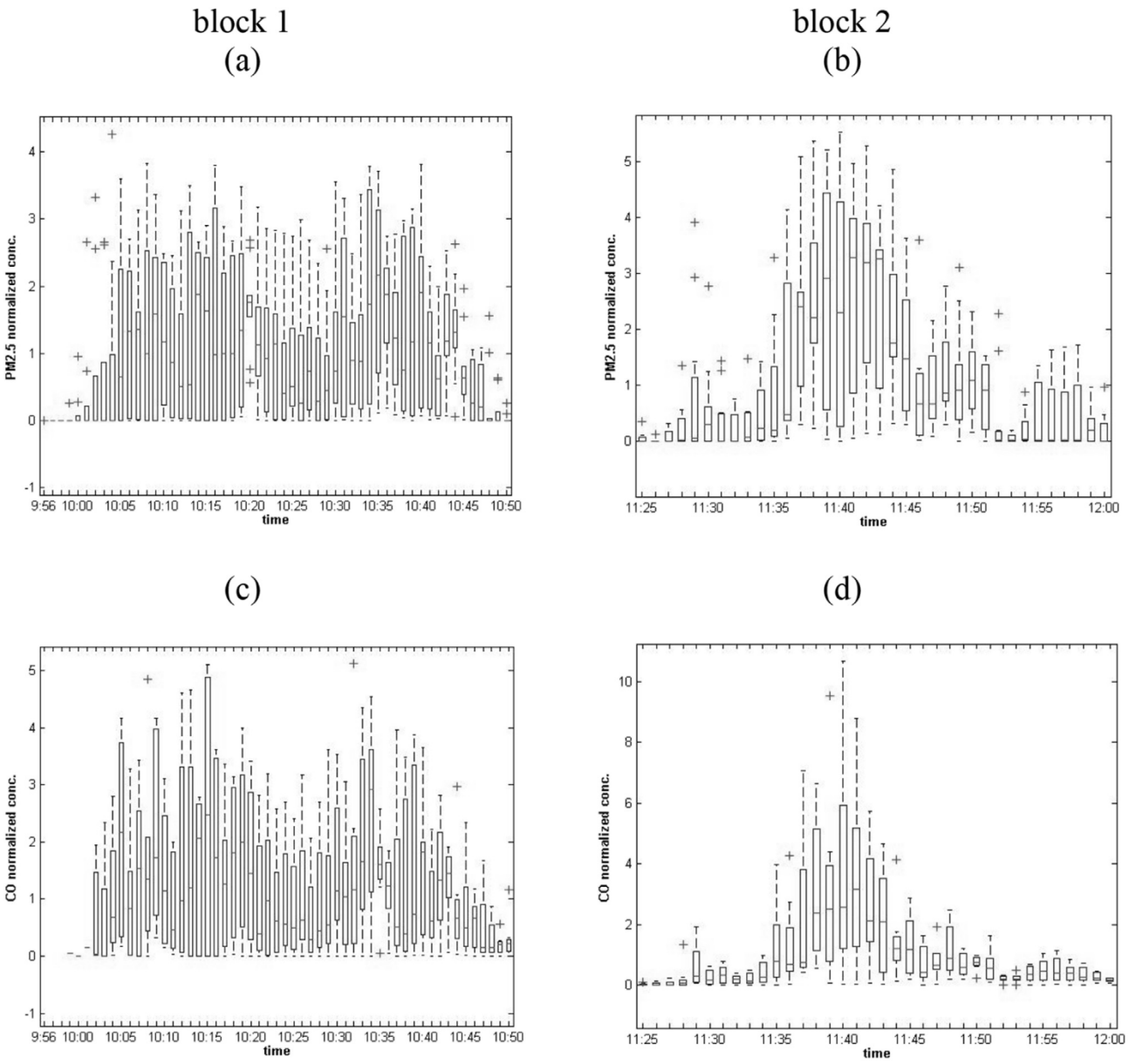

Fig. 9. Time evolution of normalized 1 min averaged PM2.5 and CO concentration. Horizontal lines show the sample medians; box limits indicate the 25th and 75th percentiles; whiskers extend to the most extreme data points not considered outliers; and the latter are represented by crosses.

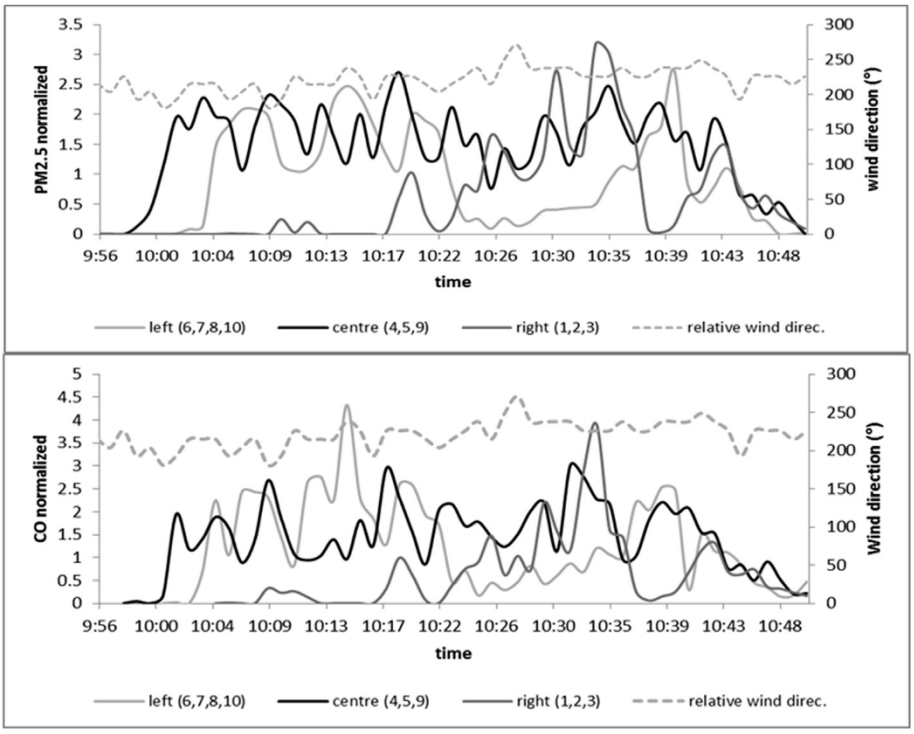

Fig. 10. Time evolution of normalized 1 min averaged PM2.5 and CO concentration by sector.

same factor explains the very low values registered during the intense flaming stage of block 2.

Additionally, a dip in the PM2.5 concentrations was observed during the flaming stage (Fig. 9a) for approximately 6 min, starting at 10:10. This was not caused by changes on the weather conditions. A decrease in smoke production is also not visible in the video recordings (at least from the observation point located in the opposite hill), nor a distinguishable (horizontal or vertical) deviation of the smoke plume, or a decrease in fire intensity. This observation indicates the difficulty posed to fire brigades chiefs in assessing the hazardous conditions of the crew based on visual observation of the plume's outer layer, from which a wrong empirical judgement could be formulated.

By grouping the sensors according to their position relating the block (see Fig. 10) it is possible to track the trajectory of the plume, or at least its lower region, during the course of the fire. As a first conclusion one can state that qualitatively both pollutants present a very similar trend along time. Also, despite no significant wind shifts in direction or wind speed, a response of the observed concentrations to surface winds is evident.

During the first 8 min from ignition, the plume is clearly oriented towards the centre of the block. At 10:02 the sensors on left side begin also to register the influence of smoke, with a peak concentration at 10:15. During this period, fire-induced turbulence creates strong oscillations in observations as a result of unstable plume behaviour and irregular trajectory. At 10:22 a shift in wind direction transports the plume to the right-hand side of the block. The fire is still very active at the moment, although the fireline is

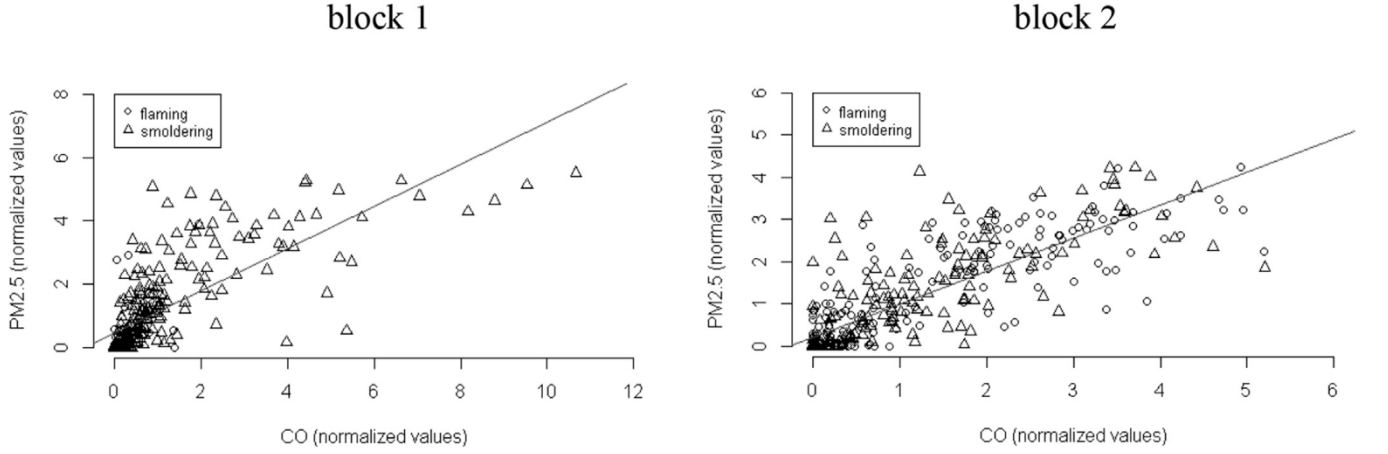

Fig. 11. Scatter plot of PM2.5 vs CO 1 min normalized concentration by fire stage. The line represents the linear model fitted to the entire duration of the experiment ('All' in Table 6). Linear models describing the PM2.5 and CO concentration pairs were calculated for each block considering the full duration of the experiment ('total') and by stage of fire. The coefficients are presented in Table 6.

close to the lower border (at the highest distance from the sensors). At 10:30, the collapse of flames induces the settling of the plume due to decreased convection. This neutrally buoyant plume leads to a widespread increase of surface levels of gas and particle, although at 10:34 left/centre downwind region starts to dominate. At 10:43, 7 min before extinction, consistent drop in concentrations occurs in all the three sectors indicating not only a progressively diminish of the emissions (associated to residual smouldering), but also a decrease in buoyancy, the latter (together with low wind intensity) causing the stagnation of the plume.

3.4.3. Correlation

The relation between the concentrations of the two pollutants was further explored using a linear regression model. The regression models were constructed with the concentration values acquired in each sensor normalized by the average of concentrations for all the sensors during the entire duration of each burn. Fig. 11 presents the scatter plot of PM2.5 vs CO normalized concentrations, for all measurements and distinguishing the fire stage (flaming or smouldering).

As indicated by Table 6, significant linear models were obtained for the relation between PM2.5 and CO concentrations (p-value < 0.0001). Block 1 presents a stronger correlation, with an R^2 of 0.69 for the entire duration of the experiment. In both blocks, the correlation changes with the combustion stage, reaching a value of approximately 0.6 in the smouldering. For the flaming phase a conclusion is hard to be extracted because of the potential effect of the reduced number of observations (55) on the low R^2 in block 2.

These results are in accordance with the regression models developed by the authors in a previous paper (Miranda et al., 2011), where similar equations for the same pair of pollutants were found for several experimental fires and wildfires. Other authors (Reinhardt and Ottmar, 2004; De Vos et al., 2009; Reisen et al., 2011) found strong correlations between respirable particles and CO in prescribed fires and wildfires, however, these results are not fully comparable since the size of respirable particles sampled was different.

4. Conclusions

It is generally accepted that firefighters are often exposed to unhealthy levels of air pollution during direct/indirect attack and mop-up on wildfires and prescribed burning, but the concentrations attained during these operations are still poorly quantified. The grid-based observations in this paper provide a better understanding of the spatial and temporal variability of PM2.5 and CO surface concentrations in the near-source region during a bushfire, highlighting the complex dynamics of particles and gas levels in a smoke plume.

Mean concentration ratios between neighbouring spots as high as 4.4 and 7.4 for PM2.5 and CO, respectively, were registered during the research burns, which were found to be largest for the smouldering combustion phase. The fact that these extreme gradients were registered within a distance of 5 m suggests that a fire crew can expect large differences in individual exposure depending on job task and position relating the smoke plume trajectory. Also, peak events of 2–3 times the mean were observed in periods exceeding 6 min.

In the two experiments the average concentrations of both PM2.5 and CO were higher during smouldering, which represents a critical risk of acute exposure, especially due to the closer proximity of firefighters to the source during mop-up, and poses an additional challenge to a successful management of the crew's safety.

Data analysis also suggests that visually estimating the fire safety conditions can be misleading, as monitored concentrations and video footage did not match well because of reduced visibility and/or inadequate view angle. These conclusions suggest that in wildfire suppression operations the safety of the involved personnel should also rely on the use of portable gas detectors for managing critical exposure to smoke. This work, in agreement with previous studies, found strong and significant correlations between CO and PM. A more detailed and complete investigation of the role of fire intensity and fuel consumption on this correlation would open the possibility to use technologically simple (this means non-expensive and reliable) and light-weighted personal CO monitors to track also the individual exposure to PM in operational conditions.

Acknowledgements

This work was supported by European Funds through COMPETE and by National Funds through the Portuguese Foundation for Science and Technology (FCT) within projects PEst-C/MAR/LA0017/2013 and FUMEXP (PTDC/AMB/66707/2006).

References

Alexander, M.E., Lanoville, R.A., 1989. Predicting Fire Behavior in the Black Spruce-lichen Woodland Fuel Type in Western and Northern Canada. Northern Forestry Centre, Edmonton, Alberta and Government of Northwest Territories, Department of Renewable Resources, Territorial Forest Fire Centre, Fort Smith, Northwest Territories, Forestry Canada.

Austin, C., 2008. Wildland Firefighter Health Risks and Respiratory Protection. Studies and Research Projects. Report R-572. Institut de recherché Robert-Sauvé en santé et en sécurité du travail (IRSST), Québec, Canada, p. 77. ISBN: 978-2-89631-297-9.

Beck, J.A., Alexander, M.E., Harvey, S.D., Beaver, A.K., 2002. Forecasting diurnal variations in fire intensity to enhance wildland firefighter safety. Int. J. Wildland Fire 11 (4), 173–182.

Byram, G.M., 1959. Combustion of forest fuels. In: Davis, K.P. (Ed.), Forest Fire: Control and Use. McGrawHill, New York, NY, pp. 61–89.

Crutzen, P.J., Andreae, M.O., 1990. Biomass burning in the tropics: impact on atmospheric chemistry and biogeochemical cycles. Science 250 (4988), 1669–1678.

De Vos, A.J.B.M., Reisen, F., Cook, A., Devine, B., Weinstein, P., 2009. Respiratory irritants in australian bushfire smoke: air toxics sampling in a smoke chamber and during prescribed burns. Arch. Environ. Contam. Toxicol. 56, 380–388.

IARC, 2010a. International Agency for Research on Cancer. IARC Monographs on the Evaluation of Carcinogenic Risks to Humans. Volume 92-Some Non-heterocyclic Polycyclic Aromatic Hydrocarbons and Some Related Exposures. Lyon, France, p. 868.

IARC, 2010b. International Agency for Research on Cancer. IARC Monographs on the Evaluation of Carcinogenic Risks to Humans. Volume 98-Painting, Firefighting, and Shiftwork. Lyon, France, p. 804.

LeMasters, G.K., Genaidy, A.M., Succop, P., Deddens, J., Sobeih, T., Barriera-Viruet, H., Dunning, K., Lockey, J., 2006. Cancer risk among firefighters: a review and meta-analysis of 32 studies. J. Occup. Environ. Med. 48 (11), 1189–1202.

Levine, J.S., 1999. Gaseous and particulate emissions released to the atmosphere from vegetation fires. In: Kee-Tai-Goh, Schwela D., Goldammer, J.G., Simpson, O. (Eds.), Health Guidelines for Vegetation Fire Events - Background Papers. United Nations Environment Programme, Nairobi, World Health Organization, Geneva, World Meteorological Organization, Geneva, Institute of Environmental Epidemiology, WHO Collaborating Centre for Environmental Epidemiology, Ministry of the Environment, Singapore, pp. 280–294.

Materna, B.L., Koshland, C.P., Harrison, R.J., 1993. Carbon monoxide exposure in wildland firefighting: a comparison of monitoring methods. Appl. Occup. Environ. Hyg. 8 (5), 479–487.

McMahon, C.K., Bush, P.B., 1992. Forest worker exposure to airborne herbicide residues in smoke from prescribed fires in the southern United-States. Am. Ind. Hyg. Assoc. J. 53 (4), 265–272.

McNamara, M.L., Noonan, C.W., Ward, T.J., 2011. Correction factor for continuous monitoring of wood smoke fine particulate matter. Aerosol Air Qual. Res. 11, 315–322.

Miranda, A.I., Ferreira, J., Valente, J., Santos, P., Amorim, J.H., Borrego, C., 2005. Smoke measurements during Gestosa 2002 experimental field fires. Int. J. Wildland Fire (IJWF) 14 (1), 107–116.

Miranda, A.I., Martins, V., Cascão, P., Amorim, J.H., Valente, J., Tavares, R., Borrego, C., Tchepel, O., Ferreira, A.J., Cordeiro, C.R., Viegas, D.X., Ribeiro, L.M., Pita, L.P., 2010. Monitoring of firefighters exposure to smoke during fire experiments in Portugal. Environ. Int. 36, 736–745.

Miranda, A.I., Borrego, C., Martins, V., Cascão, P., Amorim, J.H., Tavares, R., Valente, J., Tchepel, O., Viegas, D.X., Mário, L., Pita, P., Figueiredo, R., Davim, D., Luís, N., Oliveira, R., Cordeiro, C.R., Ferreira, A.J., Ferreira, P., Cruzeiro, C., 2011. Projecto

FUMEXP - Exposição de bombeiros ao fumo e consequentes efeitos na saúde (FUMEXP Project – Firefighters exposure and related health effects). Final report (ref.: AMB-QA-01/2011). University of Aveiro, Aveiro, Portugal. In Portuguese.

Miranda, A.I., Martins, V., Cascão, P., Amorim, J.H., Valente, J., Borrego, C., Ferreira, A.J., Cordeiro, C.R., Viegas, D.X., Ottmar, R., 2012. Wildland smoke exposure values and exhaled breath indicators on firefighters. J. Toxicol. Env. Heal A 75 (13–15), 831–843.

Ottmar, R.D., Miranda, A.I., Sandberg, D.V., 2009. Characterizing Sources of Emissions from Wildland Fires. Wildland Fires and Air Pollution (Chapter 3). Elsevier Book series: Developments in Environmental Science, pp. 61–78.

Reinhardt, T.E., Ottmar, R.D., 2000. Smoke Exposure at Western Wildfires. USDA Forest Service Pacific Northwest Research Station Research Paper, p. 525.

Reinhardt, T.E., Ottmar, R.D., 2004. Baseline measurements of smoke exposure among wildland firefighters. J. Occup. Environ. Hyg. 1, 593–606.

Reinhardt, T.E., Ottmar, R.D., Hanneman, A., 2000. Smoke Exposure Among Firefighters at Prescribed Burns in the Pacific Northwest. USDA Forest Service Pacific Northwest Research Station Research Paper 526, pp. 1–45.

Reisen, F., Brown, S.K., 2009. Australian firefighters' exposure to air toxics during bushfire burns of autumn 2005 and 2006. Environ. Int. 35, 342–352.

Reisen, F., Hansen, D., Meyer, C.P., 2011. Exposure to bushfire smoke during prescribed burns and wildfires: firefighters' exposure risks and options. Environ. Int. 37, 314–321.

Rothermel, R.C., Deeming, J.E., 1980. Measuring and Interpreting Fire Behavior for Correlation with Fire Effects. USDA Forest Service General Technical Report INT-93 November 1980.

Rothman, N., Ford, D.P., Baser, M.E., Hansen, J.A., O'Toole, T., Tockman, M.S., Strickland, P.T., 1991. Pulmonary function and respiratory symptoms in wildland firefighters. J. Occup. Med. 33 (11), 1163–1169.

TSI, 2012. SIDEPAK™ AM510 Personal Aerosol Monitor - Theory of Operation. Application note ITI-085. USA, p. 2. Available online at: http://www.tsi.com.

Viegas, D.X., Cruz, M.G., Ribeiro, L.M., Silva, A.J., Ollero, A., Arrue, B., Dios, R., Gómez-Rodríguez, F., Merino, L., Miranda, A.I., Santos, P., 2002. Gestosa fire spread experiments. In: Proceedings of the IV International Conference on Forest Fire Research/2002 Wildland Fire Safety Summit. Luso, Portugal. 16–21 November 2002.

Viegas, D.X., Palheiro, P.M., Pita, L.P., Ribeiro, L.M., Cruz, M.G., Ollero, A., Arrue, B., Dios, R.M., 2006. Analysis of fire behaviour in Mediterranean shrubs: the Gestosa fire experiments (Portugal). In: Proceedings of the V International Conference on Forest Fire Research. Figueira da Foz, Portugal. 27–30 November 2006.

Youakim, S., 2006. Risk of cancer among firefighters: a quantitative review of selected malignancies. Arch. Environ. Occup. Health 61 (5), 223–231.